

# Open Research Online

---

The Open University's repository of research publications and other research outputs

## Change-Point Analysis of Asset Price Bubbles with Power-Law Hazard Function

### Journal Item

How to cite:

Lynch, Christopher and Mestel, Benjamin (2019). Change-Point Analysis of Asset Price Bubbles with Power-Law Hazard Function. *International Journal of Theoretical and Applied Finance*, 22(7), article no. 1950033.

For guidance on citations see [FAQs](#).

© [\[not recorded\]](#)

Version: Accepted Manuscript

Link(s) to article on publisher's website:  
<http://dx.doi.org/doi:10.1142/S021902491950033X>

---

Copyright and Moral Rights for the articles on this site are retained by the individual authors and/or other copyright owners. For more information on Open Research Online's data [policy](#) on reuse of materials please consult the policies page.

---

[oro.open.ac.uk](http://oro.open.ac.uk)

International Journal of Theoretical and Applied Finance  
© World Scientific Publishing Company

## CHANGE-POINT ANALYSIS OF ASSET PRICE BUBBLES WITH POWER-LAW HAZARD FUNCTION

CHRISTOPHER LYNCH

School of Mathematics & Statistics, The Open University,  
Milton Keynes, MK7 6AA, UK  
christopher.lynch@open.ac.uk

BENJAMIN MESTEL

School of Mathematics & Statistics, The Open University,  
Milton Keynes, MK7 6AA, UK  
ben.mestel@open.ac.uk

We present a methodology to identify change-points in financial markets where the governing regime shifts from a constant rate-of-return, i.e. normal growth, to superexponential growth described by a power-law hazard rate. The latter regime corresponds, in our view, to financial bubbles driven by herding behaviour of market participants. Assuming that the time series of log-price returns of a financial index can be modelled by arithmetic Brownian motion, with an additional jump process with power-law hazard function to approximate the superexponential growth, we derive a threshold value of the hazard-function control parameter, allowing us to decide in which regime the market is more likely to be at any given time. An analysis of the Standard & Poors 500 index over the last 60 years provides evidence that the methodology has merit in identifying when a period of herding behaviour begins, and, perhaps more importantly, when it ends.

Keywords: criticality, jump process, change point, financial bubble, power laws

### 1. Introduction

When studying asset-price bubbles and anti-bubbles, a holy grail of theoreticians and practitioners alike is to predict their start and end, preferably as early as possible, so as (according to circumstances and inclination) to take maximum advantage of any opportunities that might arise or to mitigate any negative consequences or even to intervene in the market to prevent or curtail such a bubble/anti-bubble. As a result there has been a large amount of literature devoted to the detection of bubbles/anti-bubbles, with several competing approaches (see Gürkaynak 2008 and Jarrow 2016).

The valuation of stock markets, and of financial assets more generally, has been the subject of much debate. For some who favour the efficient markets hypothesis (in its various guises, including the random-walk model), bubbles fail to exist, full market knowledge having been already factored into the asset price, either immediately or sufficiently quickly to prevent any effective use of temporary market

departures from the fundamentals.

In this paper we assume the standpoint that certain periods of accelerated super-exponential growth may be viewed as financial bubbles driven by herding behaviour of market participants. Indeed, for many finance researchers and industry practitioners, the existence of asset bubbles and anti-bubbles is an established fact, a commonplace occurrence, and, indeed, many economists and practitioners question the strict application of the efficient markets hypothesis. For example, in Robertson & Wright (1998), the authors report that long-term stock returns appear to be “much less uncertain than a random-walk model would imply,” and that research suggests that there is a “weak tendency for stationary valuation indicators to predict future stock prices” so that “long-run returns can become markedly more predictable”.

Furthermore, there is a wide variety of methods used to model change-points in time series, depending on the application and research community. For example, for the econometrics community, the detection of change-points between bubbles/anti-bubbles may proceed by fitting standard time-series models such as ARIMA, (G)ARCH (Mills & Markellos 2008) and determining time points at which the nature of the models change, often using Dickey-Fuller-type tests to detect unit roots in the underlying statistical models. Several review papers discuss this approach, see, for example, Taipalus (2012), Arshanapalli & Nelson (2016), Harvey et al. (2015), Astill et al. (2017) and references therein.

There is a large body of literature in the statistics community on change-point methods, including Monte Carlo Markov Chain methods, e.g. Adams & MacKay (2007), Benson & Friel (2018), Heard & Turcotte (2017). See Aminikhanghahi & Cook (2017) for a review from the machine-learning community. The so-called Pruned Exact Linear Time (PELT) algorithm (Killick et al. 2012), a development of the method of Jackson et al. (2005), which uses both dynamic programming and pruning to produce an algorithm that is linear in the data size, is included in the R package (Killick & Eckley 2013), along with the Segment Neighbourhood algorithm, and the classical Binary Segmentation algorithm.

The approach to change-point identification taken in this paper is somewhat different from these methods. First, a normal and log-normal bi-variate distribution of growth rate and volatility is obtained empirically by fitting data from the times series over random time periods. Second, starting from an assumption that the asset grows exponentially following a geometric Brownian motion process, with superexponential growth modelled by an additional power-law hazard term (activated when a parameter  $\nu \neq 0$  following Cheah & Fry (2015)), the model is simulated using the growth rates and volatility selected randomly from the previously determined bi-variate distribution. To test whether the data fits the superexponential growth model, a most-likely-value estimate (MLV) is obtained from the distribution of  $\nu$  calculated from a maximum-likelihood estimate based on random simulation of the other model parameters. In the case studied, these MLV estimates are found empirically to be well fitted by generalised/skew logistic distributions (for both normal

and superexponential growth). The two resulting distributions are close but distinct and provide signatures for the two types of growth.

These distributions are then used as proxies for the probabilities of superexponential and normal growth themselves, and a threshold is determined which is considered as the boundary between these two regimes. Using these signature distributions, it is possible, using past and present prices, to decide, for each trading day, which is more likely to be the governing regime: superexponential growth or normal growth.

This paper is divided as follows: in §2 we present a model of returns during a financial bubble as an arithmetic Brownian motion stochastic differential equation modulated by a jump process governed by a power-law hazard function, and describe the control parameter  $\nu$ , closely following Cheah & Fry (2015). In §3 we use these defined models of normal and superexponential growth to simulate time series, and find the threshold value of the control parameter,  $\nu$ , under each regime. In §4, this threshold value is applied to the last 60 years of data from the S&P500 index and the change-points between bubble and normal market regimes are calculated. The paper concludes in §5 with suggestions for further work.

## 2. Modelling financial markets with power-law hazard rate

### 2.1. Asset price bubbles as a stochastic process

In deriving a model of periods of superexponential returns, we initially define a model for markets operating in “normal” conditions. Our first assumption is that returns on an asset-price index are log-normally distributed, and, as such, the price  $S_t$  can be modelled by the geometric stochastic differential equation

$$dS_t = \left( \mu_t + \frac{\sigma_t^2}{2} \right) S_t dt + \sigma_t S_t dW_t, \quad (2.1)$$

where  $\mu_t + \sigma_t^2/2$  is the drift coefficient,  $\sigma_t$  is the diffusion coefficient, and  $W_t$  is a standard Wiener process with  $E[W_t] = 0$  and  $E[W_t^2] = t$ . We write  $X_t = \log S_t$  and then, by applying Itô’s formula, we obtain the arithmetic Brownian motion stochastic differential equation

$$dX_t = \mu_t dt + \sigma_t dW_t. \quad (2.2)$$

Let the event  $Y$  be the occurrence of a market crash at time  $t = t_Y$ . We now follow Johansen et al. (2000) and Cheah & Fry (2015) and conjecture that in the period leading up to a crash, the asset price follows the same process as in (2.1), but suffers a deterioration in the price by a factor  $\kappa$ , where  $0 < \kappa < 1$ , at the time of a crash,  $t_Y$ . Therefore, the asset price in this regime,  $\tilde{S}$ , follows the process

$$\tilde{S}_t = S_t(1 - \kappa)^{j_t}, \quad (2.3)$$

4 Christopher Lynch & Benjamin Mestel

where  $j_t$  is the jump process

$$j_t = \begin{cases} 0 & t < t_Y, \\ 1 & t \geq t_Y. \end{cases} \quad (2.4)$$

Now, we write  $\tilde{X}_t = \log(\tilde{S}_t) = \log S_t + j_t \log(1 - \kappa)$  so that, by applying Itô's formula again, we arrive at a modified stochastic differential equation

$$d\tilde{X}_t = \mu_t dt + \sigma_t dW_t + \log(1 - \kappa) dj_t. \quad (2.5)$$

## 2.2. The hazard rate

Under the condition that event  $Y$  has not occurred up to time  $t < t_Y$ , the jump process  $j_t = 0$  and its expected value at time  $t$ ,  $E[j_t] = 0$ . Therefore, for the infinitesimally small time period  $\delta t$ ,

$$E[j_{t+\delta t} - j_t] = E[j_{t+\delta t}]. \quad (2.6)$$

The expected value of  $j_{t+\delta t}$  can be interpreted as the probability there is a crash event,  $Y$ , in the interval  $[t, t + \delta t]$  conditioned on there not having been such an event up until this point. If we define the hazard rate,  $h_t$ , as the probability per unit time that a crash event,  $Y$ , occurs in the next moment,  $\delta t$ , conditioned on it not having already happened, then

$$E[j_{t+\delta t}] = h_t \delta t. \quad (2.7)$$

Similarly, the variance of  $j_t$  conditioned on the event  $Y$  not having occurred up to time  $t$  is given by  $\text{Var}[j_t] = 0$ . Therefore, since it is clear that  $j_t = j_t^2$  we have

$$\text{Var}[j_{t+\delta t}] = h_t \delta t - h_t^2 \delta t^2. \quad (2.8)$$

## 2.3. Expectation and variance of returns in the hazard rate model

The return of an asset in the time interval  $[t, t + \delta t]$  is given by  $d\tilde{X}_t = \tilde{X}_{t+\delta t} - \tilde{X}_t$ . Since  $E[dW_t] = 0$ , it follows from (2.5) that, in a bubble regime, the expected value of the asset return in  $[t, t + \delta t]$  is

$$E[\tilde{X}_{t+\delta t} - \tilde{X}_t] = E[\mu_t \delta t] + \log(1 - \kappa) E[j_{t+\delta t} - j_t]. \quad (2.9)$$

Therefore, from (2.7) we have

$$E[\tilde{X}_{t+\delta t} - \tilde{X}_t] = \mu_t \delta t + \log(1 - \kappa) h_t \delta t. \quad (2.10)$$

Now, the expected rate of return,  $E[\tilde{X}_{t+\delta t} - \tilde{X}_t]$ , can be interpreted as the mean return over all periods of  $\delta t$  across the whole time series. Following Cheah & Fry (2015), we assume this rate of return to be a fixed value per unit time,  $\mu$ , so that

$$\mu_t = \mu - \log(1 - \kappa) h_t. \quad (2.11)$$

Since  $\log(1 - \kappa) < 0$ , Cheah & Fry (2015) interprets this to suggest that, as the risk of a crash occurring increases, the return required for traders to stay in the market must increase to compensate for the increased risk.

By a similar argument, assuming a fixed volatility  $\sigma$  across the whole time series, Cheah & Fry (2015) gives the relationship between the hazard function and the volatility as

$$\sigma_t^2 = \sigma^2 - (\log(1 - \kappa))^2 h_t \tag{2.12}$$

implying, as the authors remark, the rather counter-intuitive suggestion that as the risk of a crash increases, the volatility of the asset price actually reduces, perhaps an indication of overconfidence in the market as bubbles mature.

The theory in Cheah & Fry (2015) is valid for finite hazard rate. However, when, as in the next section, we model the hazard rate as a power law with  $h_t \rightarrow \infty$  as  $t$  approaches a critical time  $t_c$ , it is clear that equation (2.12) is problematic close to  $t_c$  because then  $\sigma_t^2 < 0$ . Note that in Johansen et al. (2000) it is assumed that  $\sigma_t = 0$  so that the stochasticity enters through the jump process, while in Cheah & Fry (2015) the full model (2.5) is presented. In this paper we take a middle position, modelling  $\mu(t)$  through (2.11), but making the ansatz  $\sigma_t = \sigma$ , a non-zero constant. While it is clear future theoretical developments might incorporate time-varying  $\sigma_t$ , the justification for our ansatz is twofold: ex ante because our focus is on the modelling of the growth rate  $\mu_t$ , and ex post because, as we shall see in §3.3, the ansatz allows the construction of a statistic that appears to discriminate ‘normal’ exponential growth from the superexponential growth that is characteristic of asset bubbles.

#### 2.4. The hazard rate as a power-law

Asset bubbles (and antibubbles) result from imitative behaviour or herding in the market. The likelihood of this imitation is a function of the general interconnectedness of the market participants, such that if  $\delta$  is the number of connections of a typical trader, one might suppose (Johansen et al. 2000) that the hazard rate satisfies  $dh_t/dt = ch_t^\delta$  with  $\delta > 1$  and  $c$  constants. Solving the differential equation with this condition gives

$$h_t = B(t_c - t)^\beta, \quad \beta = -\frac{1}{\delta - 1} < 0. \tag{2.13}$$

where  $t_c$  is a constant for which  $h_t \rightarrow \infty$  as  $t$  approaches  $t_c$ , the critical time. Importantly,  $t_c$  is considered as not being the actual time of the crash, but rather the time when the crash is most likely to happen (Johansen et al. 2000). Furthermore, we take  $\delta > 2$  so that  $-1 < \beta < 0$ , which is required for the asset to have a finite value but infinite derivative at  $t = t_c$ .

It is straightforward to see that the probability distribution function,  $P(Y_t)$ , of a crash not occurring in the interval  $(t_1, t)$ , where  $t_1$  is the initial time, is given by

$$P(Y_t) = \exp \left[ - \int_{t_1}^t h_\tau d\tau \right]. \tag{2.14}$$

6 Christopher Lynch & Benjamin Mestel

Therefore, when  $t < t_c$ ,

$$P(Y_t) = \exp \left[ \frac{B}{1 + \beta} \left( (t_c - t)^{\beta+1} - (t_c - t_1)^{\beta+1} \right) \right]. \quad (2.15)$$

We restrict  $\beta$  such that it lies within the interval  $[-1, 0)$  to prevent  $P(Y_{t_c})$  from being singular. Therefore, and it seems reasonable to suggest, there is a finite probability that the bubble ends without a crash at all. Furthermore, it follows that since it is required that  $P(Y_t)$  must lie in the interval  $[0, 1]$ , we have the additional restriction  $B \geq 0$ . Let us write  $\nu = B \log(1 - \kappa)$ , then  $\nu \leq 0$  for  $0 < \kappa < 1$ .

Now we have expressions of the statistical parameters for a market which is governed by a jump process with a power-law hazard function, and as such we can investigate how the maximum log-likelihood of these parameters behaves when applied to simulated data.

### 3. Detecting whether a market is in a bubble regime

We have developed a strategy to give a measure of the likelihood that a particular market is in a bubble regime, and in doing so find areas in observed data where the market is moving in and out of periods more likely to be exhibiting superexponential growth. The strategy is developed over the next few subsections and the implementation details are given in §4.

The first part of the strategy is to simulate normal and superexponential markets  $N$  times by building models based on the theory in §2. Let  $m = 1, \dots, N$  enumerate the models. Then each model is determined by a choice of parameters  $\mu_m, \sigma_m, \nu_m, \beta_m$  and  $t_{c,m}$ . The model is then simulated by random variation of parameters, including the initial time  $t_1$ , keeping the final time fixed. Discrete-time simulation is used with the  $n$  equally spaced times (market days), as described below. The aim is to use the simulations to obtain data from which an implied representative value  $\nu'$  can be obtained by a maximum log-likelihood estimate. It is the distribution of this representative value of  $\nu$  that is used to distinguish regimes of normal and superexponential growth.

#### 3.1. Construction of the simulated data

In order to look at the distributions of  $\nu$  as calculated in both normal and superexponential regimes, we construct large sets of simulated data for both market types, say  $N$ , allowing us to determine whether one should expect to be able to detect changes in such distributions. The simulated data for the  $m$ th time-series is constructed such that each data point is given by

$$r_i = x_i - x_{i-1} = (\mu_m - \nu_m (t_{c,m} - t_i)^{\beta_m}) \Delta + \sigma_m \sqrt{\Delta} N_i(0, 1) \quad (3.1)$$

where  $i = 1, \dots, n$ , and  $n$  is the number of trading-days worth of data in the  $m$ th time series (noting that although  $n$  varies, we keep this notation for simplicity),  $r_1 = 0$ ,  $\Delta$  is one trading-day measured in years, and the parameters indexed by  $m$

are chosen such that each simulated time-series is representative of the market in question. Here  $N_i(0, 1)$  is a standard normal distribution. In what follows we shall use this notation, sometimes indexed, to denote independent normal distributions.

Equation (3.1), which is equivalent to the differences  $r_i$  being independently distributed with probability density function

$$F(r_i, t_i) = \frac{1}{\sqrt{2\pi\sigma_{t_i}^2\Delta}} \exp\left[-\frac{(r_i - \mu_{t_i}\Delta)^2}{2\sigma_{t_i}^2\Delta}\right], \quad (3.2)$$

is derived from (2.5) and (2.11). In what follows we will restrict  $\sigma$  at a constant value, to reduce the complexity of the maximum log-likelihood calculations in §3.2.

We note that  $-1 < \beta_m < 0$  so that we take  $\beta_m \sim U(-1, 0)$ , a uniform distribution on  $(-1, 0)$ . As for  $t_c$ , we know that should occur after the time  $t_n$ . We take  $t_c \sim U(t_n, t_n + \gamma)$  where  $\gamma$  is a short time, as described below in §3.2.

The distributions for  $\mu_m$  and  $\sigma_m$  maybe be taken from the observed data of the target market as described in §3.1.1. This leaves us to consider how to sample  $\nu_m$ . It is not immediately apparent how these values should be distributed, but a closer look at (2.15) can point us in the right direction. The distribution of  $\nu_m$  is discussed in §3.1.2.

### 3.1.1. Estimating distributions for $\mu_m$ and $\sigma_m$

Since the aim is to create realistic simulated data for the particular market being the focus of our investigations, we need to derive realistic samples of both the drift parameter,  $\mu_m$ , and its standard deviation,  $\sigma_m$  to be used in building the model.

In this section we have taken, as an example, the S&P500 index. We have taken market close data from January 1950 to June 2018 and calculated the daily mean of the log-price return,  $\mu_m\Delta$ , and its standard deviation,  $\sigma_m\sqrt{\Delta}$  for a large sample (10,000) of randomly chosen time periods (in years) of lengths drawn from  $U(0, 10)$ .

As can be seen from Fig. 1, we have fitted approximate normal distributions to these sample data for  $\mu_m\Delta$  and  $\log(\sigma_m\sqrt{\Delta})$  and in Fig. 2 we have derived a simulated joint distribution of the daily mean of the log-price returns. This joint distribution is used in the construction of the simulated data on which we have based our subsequent analysis of this particular time series, as described in §4.

It is important to note that we have not attempted to accurately model the distribution of the daily means and standard deviations; rather our aim has been to capture the approximate range and frequency of values observed in this particular market.

### 3.1.2. Estimating a realistic distribution of $\nu_m$

In order to decide upon a realistic distribution of  $\nu_m$  to be used in generating our simulated data, we must first be clear on which distributions are reasonable for both  $B$  and  $\kappa$ . First, looking at (2.15), we know that at time  $t = t_c$  the probability that



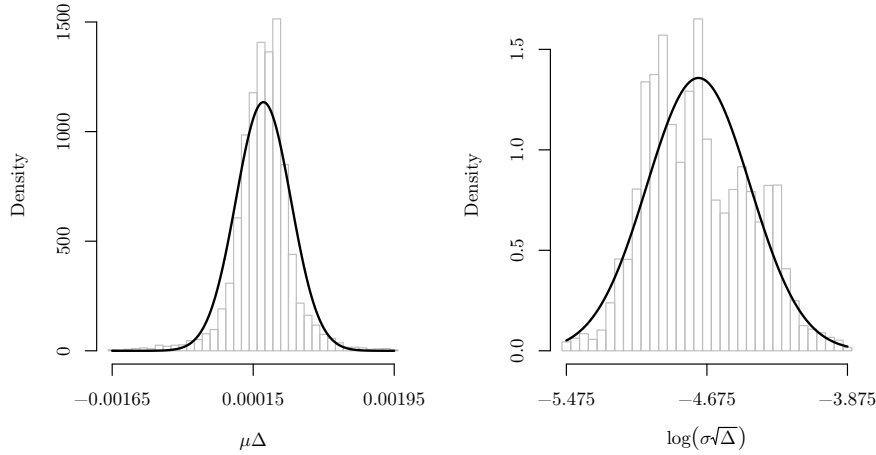


Fig. 1. Distribution of daily mean (not annualised) and the logarithm of their standard deviations derived from the S&P500 index log-price returns from January 1950 to June 2018. 10,000 sample time-windows were taken with spans up to 10 years drawn randomly from  $U(0, 10)$ . The returns and logarithm of their standard deviations have been fitted with normal distributions. As can be seen, the fits are fair and sufficient for the purposes of building market simulations which are at least representative of historical reality.

a crash has not occurred up until this point is given by

$$P(Y_{t_c}) = \exp \left[ -\frac{B}{1 + \beta} (t_c - t_1)^{1+\beta} \right]. \quad (3.3)$$

Since we chose  $\beta \sim U(-1, 0)$ , and defining the random variable  $\tilde{p} = P(Y_{t_c})$ , for which, without any other prior knowledge, we take  $\tilde{p} \sim U(0, 1)$ , the probability density function of  $B$  can be found by considering the relationship between  $\beta$  and  $B$  given by

$$B = -(\beta + 1)\theta^{-(\beta+1)} \log \tilde{p}, \quad (3.4)$$

where  $\theta = t_c - t_1$ .

First, we consider the function  $g(\theta, \beta) = (\beta + 1)\theta^{-(\beta+1)}$  and its partial derivative with respect to  $\beta$ ,

$$\frac{\partial g}{\partial \beta} = \theta^{-(\beta+1)}(1 - (\beta + 1) \log \theta), \quad \theta > 0. \quad (3.5)$$

It can be seen that the function  $g(\theta, \beta)$  has a unique turning point where  $\theta = \exp[1/(\beta + 1)]$ . However, since  $-1 \leq \beta \leq 0$ , a zero of  $\partial g/\partial \beta$  only exists when  $\theta \geq e$ , and for  $0 < \theta \leq e$  the function  $g(\theta, \beta)$  is monotonically increasing as a function of  $\beta$ .

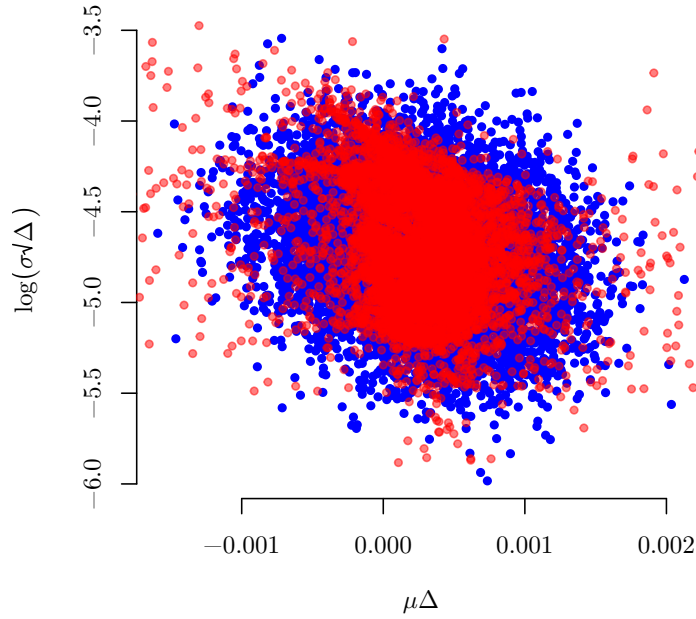


Fig. 2. Joint distributions of daily  $\mu\Delta$  and  $\log(\sigma\sqrt{\Delta})$  for the S&P500 index. In red are 10,000 points of observed data taken from the log-price returns of the index between January 1950 and June 2018, and in blue is the fitted bi-variate normal distribution used for simulating data series using the model given in (3.1). There is an amount of negative correlation between the two parameters, given by a correlation coefficient of  $-0.25$ .

Now, we consider that the random variable  $B$  takes a particular value  $B = b$  where  $b \geq 0$ . By rearranging (3.4) and writing  $\tilde{p} = p_b(\beta)$  when  $B = b$ , we have

$$p_b(\beta) = \exp\left(-\frac{b}{g(\theta, \beta)}\right). \quad (3.6)$$

Since  $g(\theta, \beta)$  increases monotonically as a function of  $\beta$  for  $0 < \theta \leq e$ , this is also true for  $p_b(\beta)$ . Furthermore, since there is a unique turning point of  $g(\theta, \beta)$  while  $\theta > e$  this is similarly true for  $p_b(\beta)$ . These two cases are shown in Fig. 3(a) and Fig. 3(b) respectively.

Now, since  $B = -g(\theta, \beta) \log \tilde{p}$ , for a fixed value of  $\beta$ , in the two cases  $0 < \theta \leq e$  and  $\theta > e$ ,  $B$  is a monotonically decreasing function of  $\tilde{p}$ . Therefore, we can see that the Cumulative Distribution Function of  $B$ ,  $F_B(b) = P(B \leq b)$ , can be expressed as

$$P(B \leq b) = 1 - P(B > b) = 1 - \int_{-1}^0 p_b(\beta) d\beta. \quad (3.7)$$

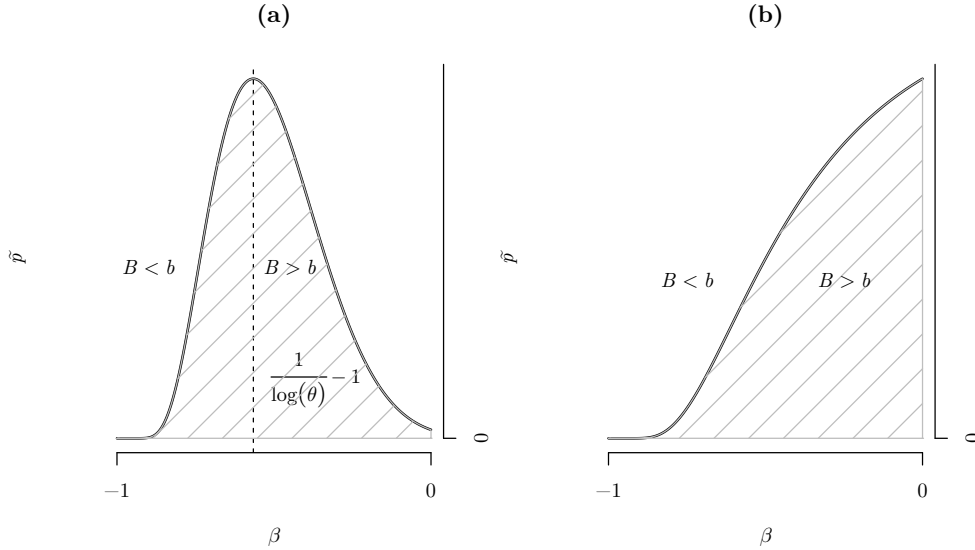


Fig. 3. Here is shown, for a given value of  $b$ , the relationship between  $\tilde{p}$  and  $\beta$  for which where  $B = b$ , in the two cases (a)  $\theta > e$ , and (b)  $0 < \theta \leq e$ , where  $\theta$  is the time between the start of the observed data and the critical time  $t_c$ . Since  $0 \leq \tilde{p} \leq 1$ , in both cases the probability that  $B < b$  is the area above the curve bounded by  $\tilde{p} \leq 1$ . Deriving an expression for this area gives the probability density function for  $B$  for a given value of  $\theta$ .

Therefore the probability density function of  $B$  can then be found by

$$\begin{aligned}
 f_B(b) &= -\frac{d}{db} \int_{-1}^0 p_b(\beta) d\beta \\
 &= \int_0^1 \frac{1}{(1-\rho)\theta^{\rho-1}} \exp\left(-\frac{b}{(1-\rho)\theta^{\rho-1}}\right) d\rho,
 \end{aligned} \tag{3.8}$$

where  $\rho = -\beta$ . To simplify matters a little further for the purposes of constructing the simulated data on which to test the bubble detection method, we assume that the time between the critical time,  $t_c$ , and the last date in the observed data is small compared to the time span of the data set so that the probability density function becomes

$$f_B(b) = \int_0^1 \frac{1}{(1-\rho)\hat{\theta}^{\rho-1}} \exp\left(-\frac{b}{(1-\rho)\hat{\theta}^{\rho-1}}\right) d\rho, \tag{3.9}$$

where  $\hat{\theta}$  is the time span of the observed data.

The distribution of the “expected” percentage fall in the market upon the occurrence of a crash,  $\kappa$ , is difficult to determine since market crashes are, on the one hand, rare and, on the other, not subject to strict definition. Here we model it by a

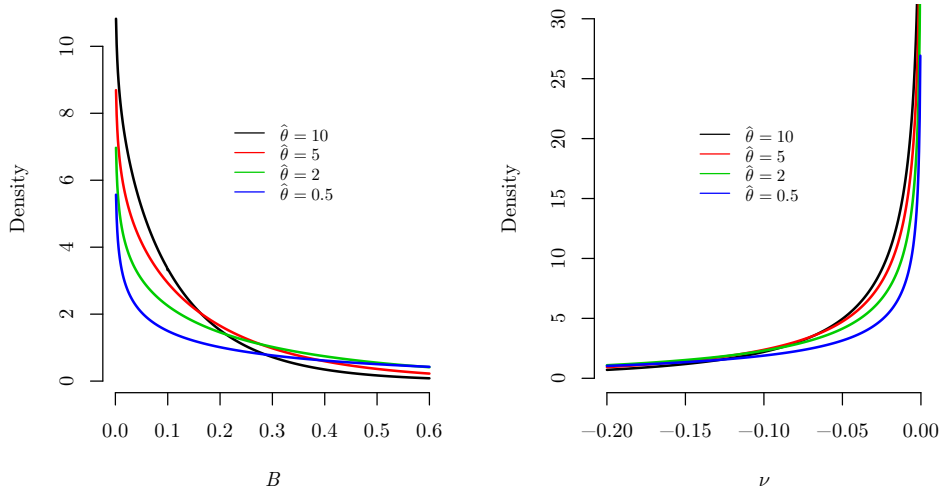


Fig. 4. Distribution of  $B$  on the left and, on the right, the distribution of  $\nu$  given from (3.9) and (3.10) respectively, for varying values of the observed data time span,  $\hat{\theta}$ , assuming that the difference between the time  $t_c$  and the last date of the observed data is small compared to the total time span. The distribution of  $\nu$  further assumes that the fraction of the market fall in the event of a crash is a uniform random variable  $\kappa \sim U(0, 0.75)$ .

uniformly distributed random variable  $\kappa \sim U(0, 0.75)$ . Other choices of upper limit are certainly possible, and 0.75 may appear somewhat high since a price fall of 75% is unlikely to occur in practice. However since the value of  $\kappa$  is an expectation of draw-down if indeed a crash does happen, we should not necessarily take it as being representative of draw-downs which have happened in the real world.

The distribution of the random variable  $\nu = B \log(1 - \kappa)$  can be written as

$$f_\nu(\nu) = - \int_0^{\kappa_+} \frac{1}{\kappa_+ \log(1 - \kappa)} f_B\left(\frac{\nu}{\log(1 - \kappa)}\right) d\kappa, \quad (3.10)$$

where  $\kappa_+ = 0.75$ . The probability density functions  $f_B$  and  $f_\nu$  are shown in Fig. 4. We can obtain the the parameter  $\nu_m$  by sampling from the distribution  $f_\nu$ .

### 3.2. Maximum log-likelihood analysis of the power-law hazard function

Now that a model has been built which can generate simulated data  $x_1, \dots, x_n$  via (3.1) we now describe how these data, and in particular, the log returns  $r_1, \dots, r_n$ , given by  $r_1 = 0$ , and  $r_i = x_i - x_{i-1}$ , for  $i = 1, \dots, n$ , may be used to obtain maximum log-likelihood estimates for  $\nu$ .

Equation (3.2) describes the probability density function of the log-price returns as normally distributed parametrised by time-dependent drift and variance terms.

12 Christopher Lynch & Benjamin Mestel

Now, given a set of observed asset log-price returns, model parameters may be estimated using maximum log-likelihood methods; however, to simplify the analysis and allow the parameter  $\nu$  to be found explicitly, we hold the variance,  $\sigma_t^2$ , as a constant such that  $\sigma_t^2 = \sigma^2$  giving the simplified probability density function,  $\tilde{F}(r, t)$ , as

$$\tilde{F}(r_i, t_i) = \frac{1}{\sqrt{2\pi\sigma^2\Delta}} \exp \left[ -\frac{(r_i - \Delta(\mu - \nu(t_c - t_i)^\beta))^2}{2\sigma^2\Delta} \right], \quad (3.11)$$

so that

$$\log \left( \tilde{F}(r_i, t_i) \right) = -\frac{1}{2} \log(2\pi\Delta) - \log \sigma - \frac{(r_i - \Delta(\mu - \nu(t_c - t_i)^\beta))^2}{2\sigma^2\Delta}. \quad (3.12)$$

Therefore, given a series of log-price returns,  $R = (r_1, r_2, \dots, r_n)$  and times  $T = (t_1, t_2, \dots, t_n)$ , the log-likelihood function of the parameters is given by

$$\log \mathcal{L}(\mu, \sigma, \nu, t_c, \beta; R) = -\frac{n}{2} \log(2\pi\Delta) - n \log \sigma - \sum_{i=1}^n \frac{(r_i - \Delta(\mu - \nu(t_c - t_i)^\beta))^2}{2\sigma^2\Delta}. \quad (3.13)$$

Given this simplified equation, it is possible to find the maximum log-likelihood explicitly for the parameters,  $\mu, \sigma$ , and  $\nu$ . We have labelled these as the linear parameters, and  $t_c$  and  $\beta$  as nonlinear and we derive expressions to find the value of each parameter that maximises the log-likelihood function, and which are, therefore, the most likely true values which generate the observed data.

Linear parameters. Starting with the parameters  $\mu$  and  $\nu$ , the values,  $\mu'$  and  $\nu'$ , which maximise the log-likelihood function are found by forming the partial derivatives

$$\begin{aligned} \frac{\partial}{\partial \nu} \log \mathcal{L} &= -\frac{1}{\sigma^2} \sum_{i=1}^n (t_c - t_i)^\beta (r_i - \Delta(\mu - \nu(t_c - t_i)^\beta)) = 0 \\ \frac{\partial}{\partial \mu} \log \mathcal{L} &= \frac{1}{\sigma^2} \sum_{i=1}^n (r_i - \Delta(\mu - \nu(t_c - t_i)^\beta)) = 0 \end{aligned} \quad (3.14)$$

and, as such, are given uniquely by

$$\mu' = \frac{c_1 c_2 - n c_3 \bar{R}}{\Delta c_4}, \quad \nu' = \frac{n(c_2 - c_1 \bar{R})}{\Delta c_4}, \quad (3.15)$$

where

$$c_1 = \sum_{i=1}^n (t_c - t_i)^\beta, \quad c_2 = \sum_{i=1}^n (t_c - t_i)^\beta r_i, \quad c_3 = \sum_{i=1}^n (t_c - t_i)^{2\beta} \quad (3.16)$$

and

$$\bar{R} = \frac{1}{n} \sum_{i=1}^n r_i, \quad c_4 = c_1^2 - n c_3. \quad (3.17)$$

Finally, the partial derivative of the log-likelihood function with respect to  $\sigma$  is

$$\frac{\partial}{\partial \sigma} \log \mathcal{L} = -\frac{n}{\sigma} + \frac{1}{\sigma^3 \Delta} \sum_{i=1}^n (r_i - \Delta(\mu - \nu(t_c - t_i)^\beta))^2 = 0, \quad (3.18)$$

so that  $\sigma'^2$  can be explicitly expressed as

$$\sigma'^2 = \frac{1}{n\Delta} \sum_{i=1}^n (r_i - \Delta(\mu' - \nu'(t_c - t_i)^\beta))^2. \quad (3.19)$$

Since the value which maximises the log-likelihood function for each of the linear parameters may be determined uniquely for given values of  $t_c$  and  $\beta$ , it is necessary to first determine the maximising values  $t'_c$  and  $\beta'$ .

Non-linear parameters. By differentiating with respect to  $t_c$  and  $\beta$ , the non-linear parameters must satisfy

$$\frac{\nu' \beta}{\sigma'^2} \sum_{i=1}^n \frac{1}{t_c - t_i} (\Delta (\mu'(t_c - t_i)^\beta - \nu'(t_c - t_i)^{2\beta}) - r_i(t_c - t_i)^\beta) = 0 \quad (3.20)$$

and

$$\frac{\nu'}{\sigma'^2} \sum_{i=1}^n \log(t_c - t_i) (\Delta (\mu'(t_c - t_i)^\beta - \nu'(t_c - t_i)^{2\beta}) - r_i(t_c - t_i)^\beta) = 0. \quad (3.21)$$

It can be seen that it is not possible to determine these nonlinear parameters explicitly. However, we do know something about their constraints. First, it is necessary that  $-1 < \beta < 0$  such that the probability of a crash occurring, on the condition that it has not already happened, remains finite. As for  $t_c$ , we know that it should occur after the time  $t_n$ , for the same reason. Furthermore, if  $t_c$  is very far away from  $t$ , it is unlikely that the effect of the power-law would be detectable. Therefore, we can sample values of  $\beta \sim U(-1, 0)$  and  $t_c \sim U(t, t + \gamma)$  where  $\gamma$  is a short time interval, and derive distributions for  $\mu'$  and  $\sigma'$ , but more importantly for  $\nu'$ . In what follows, we take  $\gamma = 0.5$  year.

### 3.3. Maximum log-likelihood analysis of $\nu$ in simulated data

#### 3.3.1. $\nu'$ distribution

Equations (3.15) give  $\mu'$  and  $\nu'$  from the maximum log-likelihood estimates, given a simulated set of log returns  $R = (r_1, r_2, \dots, r_n)$  observed at times  $T = (t_1, t_2, \dots, t_n)$ . Recall from the beginning of §3 that we build  $N$  models, with the  $m$ th model given by (3.1). In what follows, we take the returns data  $r_{i,m}$ ,  $i = 1, \dots, n$  for the  $m$ th model to input into a simulation where  $n$ ,  $t_c$  and  $\beta$  are random variables which are independent of the model chosen. We therefore must modify the maximum log-likelihood estimates slightly to take into account the difference between the model generating the log returns data and that being used in the simulation. Specifically, we use (3.13) to obtain the maximum log-likelihood estimates for  $\nu$

14 Christopher Lynch & Benjamin Mestel

(and  $\mu$ ), with  $r_i = r_{i,m}$ ,  $i = 1, \dots, n$ , where  $n$  is the (randomly varying) length of the time series.

Recall from (3.14) that a time series of log-price returns  $R = (r_1, r_2, \dots, r_n)$  observed at times  $T = (t_1, t_2, \dots, t_n)$ , the values of  $\nu'$  and  $\mu'$  that maximise their respective log-likelihoods are given by

$$\begin{aligned}\nu' &= \frac{\mu' \sum_{i=1}^n (t_c - t_i)^\beta - \Delta^{-1} \sum_{i=1}^n (t_c - t_i)^\beta r_i}{\sum_{i=1}^n (t_c - t_i)^{2\beta}} \\ \mu' &= \frac{\nu'}{n} \sum_{i=1}^n (t_c - t_i)^\beta + \Delta^{-1} \frac{1}{n} \sum_{i=1}^n r_i.\end{aligned}\quad (3.22)$$

Setting  $r_i = r_{i,m}$ , the sum of the simulated log-price returns is given by

$$\begin{aligned}\sum_{i=1}^n r_{i,m} &= \sum_{i=1}^n \left( (\mu_m - \nu_m (t_{c,m} - t_i)^{\beta_m}) \Delta + \sigma_m \sqrt{\Delta} N_i(0, 1) \right) \\ &= n\mu_m \Delta - \nu_m \Delta k_1 + \sum_{i=1}^n \sigma_m \sqrt{\Delta} N_i(0, 1),\end{aligned}\quad (3.23)$$

where  $k_1 = \sum_{i=1}^n (t_{c,m} - t_i)^{\beta_m}$ . Recalling the notation in (3.16), and substituting into equation (3.22), we have

$$\begin{aligned}\mu' &= \frac{\nu' c_1}{n} + \frac{1}{n} \left( n\mu_m - \nu_m k_1 + \sum_{i=1}^n \frac{\sigma_m}{\sqrt{\Delta}} N_i(0, 1) \right) \\ &= \mu_m + \frac{1}{n} (c_1 \nu' - k_1 \nu_m) + S_1,\end{aligned}\quad (3.24)$$

where  $S_1 = \frac{1}{n} \sum_{i=1}^n \frac{\sigma_m}{\sqrt{\Delta}} N_i(0, 1)$ . Furthermore,

$$\begin{aligned}\nu' &= \frac{1}{c_3} \left( \mu' c_1 - \mu_m c_1 + \nu_m k_3 - \sum_{i=1}^n \frac{\sigma_m}{\sqrt{\Delta}} (t_c - t_i)^\beta N_i(0, 1) \right) \\ &= \frac{k_3}{c_3} \nu_m + \frac{c_1}{c_3} (\mu' - \mu_m) - S_2,\end{aligned}\quad (3.25)$$

where  $S_2 = \frac{1}{c_3} \sum_{i=1}^n \frac{\sigma_m}{\sqrt{\Delta}} (t_c - t_i)^\beta N_i(0, 1)$  and  $k_3 = \sum_{i=1}^n (t_c - t_i)^\beta (t_{c,m} - t_i)^{\beta_m}$ . Now, solving for  $\nu'$ ,

$$\nu' = \frac{1}{nc_3 - c_1^2} ((k_3 n - c_1 k_1) \nu_m - n(c_3 S_2 - c_1 S_1)). \quad (3.26)$$

However

$$\begin{aligned}c_3 S_2 - c_1 S_1 &= \sum_{i=1}^n \left( \frac{\sigma_m}{\sqrt{\Delta}} (t_c - t_i)^\beta - \frac{c_1 \sigma_m}{\sqrt{\Delta} n} \right) N_i(0, 1) \\ &= N_m(0, 1) \frac{\sigma_m}{\sqrt{\Delta}} \sqrt{\left( c_3 - \frac{c_1^2}{n} \right)},\end{aligned}\quad (3.27)$$

where  $N_m(0, 1)$  is a single normally distributed random variable. Therefore

$$\nu' = \frac{1}{nc_3 - c_1^2} \left( (k_3n - c_1k_1)\nu_m - nN_m(0, 1) \sigma_m \sqrt{\frac{1}{\Delta} \left( c_3 - \frac{c_1^2}{n} \right)} \right). \quad (3.28)$$

Furthermore, for analysis of simulated data that follow a Brownian motion stochastic differential equation, we simply set  $\nu_m = 0$  and (3.28) becomes

$$\nu' = N_m(0, 1) \frac{\sigma_m}{\sqrt{\Delta \left( c_3 - \frac{c_1^2}{n} \right)}}. \quad (3.29)$$

Note that, although  $\nu_m \leq 0$ , there is no such restriction in the distribution of  $\nu'$ , because random variation may cause the maximum log-likelihood estimate to correspond to negative growth, even when  $\nu_m < 0$ . In fact, as is to be expected, the distribution in the case of superexponential growth falls principally on negative values of  $\nu'$ , but for  $\nu_m = 0$ , the distribution is symmetric about  $\nu' = 0$ .

#### 3.4. Approximations for large $N$

Given the large number,  $N$ , of models needed to derive a properly representative picture of the distributions of  $\nu'$ , it is important to approximate the sums in (3.28) and (3.29) to reduce the computing time required.

Replacing the sums with integral approximations, it is straightforward to obtain

$$c_1 = \sum_{i=1}^n (t_c - t_i)^\beta \approx \hat{c}_1 = \frac{1}{\Delta} \frac{(t_c - t_1)^{\beta+1} - (t_c - t_n)^{\beta+1}}{\beta + 1} \quad (3.30)$$

$$c_3 = \sum_{i=1}^n (t_c - t_i)^{2\beta} \approx \hat{c}_3 = \frac{1}{\Delta} \frac{(t_c - t_1)^{2\beta+1} - (t_c - t_n)^{2\beta+1}}{2\beta + 1} \quad (3.31)$$

$$k_1 = \sum_{i=1}^n (t_{c,m} - t_i)^{\beta_m} \approx \hat{k}_1 = \frac{1}{\Delta} \frac{(t_{c,m} - t_1)^{\beta_m+1} - (t_{c,m} - t_n)^{\beta_m+1}}{\beta_m + 1}. \quad (3.32)$$

An approximation to  $k_3$ , of order  $a \geq 0$ , is

$$\hat{k}_3 = \frac{1}{\Delta} \begin{cases} \sum_{j=0}^a \binom{\beta_m}{j} (t_{c,m} - t_c)^j \frac{(t_c - t_1)^{\alpha_m - j + 1} - (t_c - t_n)^{\alpha_m - j + 1}}{\alpha_m - j + 1} & t_{c,m} < t_c \\ \frac{(t_c - t_1)^{\alpha_m + 1} - (t_c - t_n)^{\alpha_m + 1}}{\alpha_m + 1} & t_{c,m} = t_c \\ \sum_{j=0}^a \binom{\beta}{j} (t_c - t_{c,m})^j \frac{(t_{c,m} - t_1)^{\alpha_m - j + 1} - (t_{c,m} - t_n)^{\alpha_m - j + 1}}{\alpha_m - j + 1} & t_{c,m} > t_c \end{cases}$$

where  $\alpha_m = \beta + \beta_m$ .

Using these approximations, which work remarkably well in practice, the expressions for  $\nu'$  in (3.28) and (3.29) become

$$\nu' = \frac{1}{n\hat{c}_3 - \hat{c}_1^2} \left( (\hat{k}_3n - \hat{c}_1\hat{k}_1)\nu_m - nN_m(0, 1) \sigma_m \sqrt{\frac{1}{\Delta} \left( \hat{c}_3 - \frac{\hat{c}_1^2}{n} \right)} \right) \quad (3.33)$$



16 Christopher Lynch & Benjamin Mestel

and

$$\nu' = N_m(0, 1) \frac{\sigma_m}{\sqrt{\Delta \left( \hat{c}_3 - \frac{\hat{c}_1^2}{n} \right)}}. \quad (3.34)$$

### 3.4.1. Example fitted distributions of $\nu'$ most likely value

Let us now briefly take stock of the development thus far. For each of  $m = 1, \dots, N$  we have randomly selected parameters  $\mu_m, \sigma_m, \nu_m, \beta_m$  and  $t_{c,m}$ . Now for each of these parameter choices, we simulate the model by taking a large random sample of times  $t_1, \dots, t_n$ , with  $t_n$  fixed but  $n$ , and hence  $t_1$ , varying randomly, and of parameters  $\beta \sim U(-1, 0)$  and  $t_c \sim U(t_n, t_n + \gamma)$ , so that the returns  $r_1, \dots, r_n$  are obtained from (3.1).

For each of these simulated data series, we can find distributions of  $\nu'$  given sufficient samples drawn for the controlling random variables,  $\beta$  and  $t_c$ . However, since the MLEs in (3.15) are highly biased, in that the expected value of  $\nu'$  may diverge from the simulated parameter value, we take the most likely value of these distributions, rather than the expected value, as an estimate of the parameter value. We investigate how the most likely values of these distributions are themselves distributed over many thousands of simulated data series. We define the most likely value of the distribution of  $\nu'$  as  $\bar{\nu}$ .

As an example, Fig. 5 shows the resulting distribution for  $\bar{\nu}$  for the normal and superexponential growth cases taken from sample data drawn from the S&P500 index over the past 60 years, as used in section 4. In this figure, the distributions are overlaid with, in both cases, the generalised/skew forms of the Cauchy, normal, Laplace and logistic distributions. These fits were obtained by the `fitdistrplus` package as used in the statistical computing platform, R. In Table 3.4.1 we give summary statistics for all fitted distributions.

By all standard measures, the generalised logistic distributions are the best fits, with none of the other distributions not being rejected at the 5% level for the Kolmogorov-Smirnov test. Although these fits are clearly not exact around the modal value, there is remarkably good agreement with 5000 data points. In the normal and superexponential cases the fits cannot be rejected in a Kolmogorov-Smirnov (KS) test at the 5% level.

A better fit may be possible using a distribution that truncates the (generalised) logistic distribution, but a more refined fit is unlikely to improve the application to financial indices, as the distribution of  $\mu_m \Delta$  and  $\log(\sigma_m \sqrt{\Delta})$  is only approximated by the bi-normal distribution in equation (3.1).

### 3.4.2. Threshold value of $\bar{\nu}$

In order to determine whether a particular time series is in a normal or superexponential growth regime we have decided to take a Bayesian approach to hypothesis

Measure	Normal			
	Logistic	Laplace	Cauchy	Normal
AIC	9954	10151	11324	10142
BIC	9974	10171	11344	10162
KS $p$ -value	0.0059	0.0366	0.0652	0.0275
KS test	not rejected	rejected	rejected	rejected
Measure	Superexponential			
	Logistic	Laplace	Cauchy	Normal
AIC	11448	11504	12473	12204
BIC	11467	11524	12492	12224
KS $p$ -value	0.0188	0.0321	0.0585	0.0695
KS test	not rejected	rejected	rejected	rejected

Table 1. Simulated data  $\bar{\nu}$  distribution fitting statistics, showing the generalised/skew logistic distributions to be the best fits for both normal and superexponential growth.

testing such that we have two potential hypotheses:  $H_1$  being the case in which the most likely value,  $\bar{\nu}$ , indicates a superexponential governing regime, and  $H_0$ , the case in which  $\bar{\nu}$  indicates the market is following a normal growth period. We accept  $H_1$  and reject  $H_0$  when  $P(H_1|\bar{\nu}) > P(H_0|\bar{\nu})$ . Since  $P(H_i|\bar{\nu}) = f_{H_i}(\bar{\nu})P(H_i)/P(\bar{\nu})$ , where  $f_{H_i}(\bar{\nu})$  is the probability density function of  $\bar{\nu}$  given the underlying hypothesis, we accept  $H_1$  when

$$f_{H_1}(\bar{\nu}) > f_{H_0}(\bar{\nu}) \frac{P(H_0)}{P(H_1)}. \tag{3.35}$$

Assuming that the probability of the governing regime being superexponential  $P(H_1) = p$ , the threshold is the value of  $\bar{\nu}$  for which

$$f_{H_1}(\bar{\nu}) = f_{H_0}(\bar{\nu}) \frac{1-p}{p}. \tag{3.36}$$

We have no prior knowledge of the value of  $p$ , and have assumed a value of 0.5 such that the threshold value,  $\bar{\nu}_T$  is given by the solution of  $f_{H_1}(\bar{\nu}) = f_{H_0}(\bar{\nu})$ . Therefore, when applying this threshold to market data, by calculating the most likely value of the log-likelihood maximising distribution of  $\nu'$  for a particular time period, we can simply say that this regime is more probably in a normal growth phase if  $\bar{\nu} > \bar{\nu}_T$  where  $\bar{\nu}_T$  is the threshold value calculated from the simulations of  $H_1$  and  $H_0$  derived from the statistical parameters of the market in question.

#### 4. Applying $\bar{\nu}_T$ log-likelihood threshold to S&P500 index

We have used the methodology developed in the preceding sections to examine the S&P500 index from January 1960 up to June 2018, to determine whether the

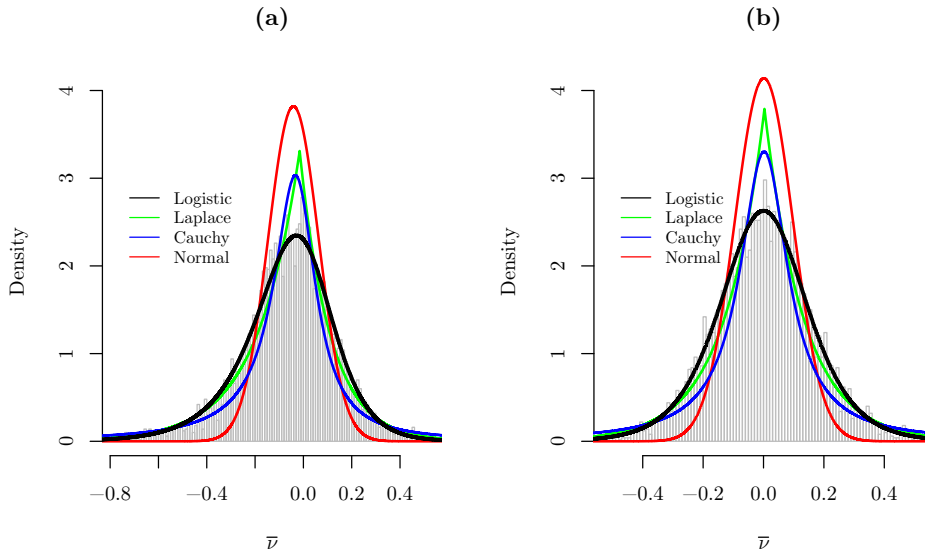


Fig. 5. Distributions of  $\bar{v}$ , given the experimental simulations of the (a) superexponential and (b) normal regimes. Having trialled a number of candidate distributions against the experimental data, a generalised logistic distribution appears to fit the data well for both the normal and superexponential governing regimes.

market is exhibiting superexponential growth at any particular time. The precise algorithm for the calculation of the distribution of  $\bar{v}$  and of the threshold value  $\bar{v}_T$  is somewhat involved and is described below as a sequence of steps. Some of these steps have been described earlier by way of example of the theory, but are included here for completeness.

Gather market data for simulations. Taking the S&P500 index from 1950, the (daily) log-returns were calculated. Random time spans of up to 10 years with random starting points (consistent with the period January 1950 – June 2018) were sampled and on each of these random intervals the mean daily log return  $\mu\Delta$  and its standard deviation  $\sigma\sqrt{\Delta}$  were calculated and fitted to a bi-variate normal distribution. In this study, 10,000 random intervals were taken. In Fig. 2, a comparison of the data and fitted distribution is illustrated, showing fair agreement between the model and the data.

Simulate market regimes to find  $\bar{v}$  distribution. The second stage is to simulate log-returns using the stochastic models for normal and superexponential growth. Taking the arbitrary, but convenient 10-year period 1980 – 1990, a stochastic model was built, and simulated data for each of the two cases were generated, as described

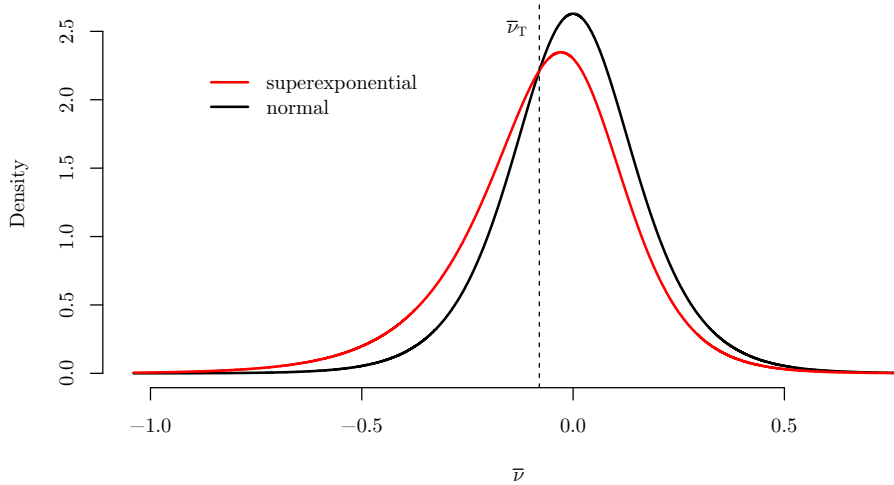


Fig. 6. A comparison of the logistic fitted distributions of the superexponential and normal regimes. The threshold value  $\bar{\nu}_T$  is interpreted as the lower bound on the value of  $\bar{\nu}$  at which one should expect the governing regime to be normal. This makes the assumption that the probability of the regime being in one of the two possible regimes is 0.5.

below.

Normal growth. 5000 simulations were built for normal growth by randomly choosing  $\mu_m, \sigma_m$  via the bi-variate normal distribution given above,  $t_{c,m}$  from the uniform distribution  $U(1990, 1990.5)$  and  $\beta_m$  from the uniform distribution  $U(-1, 0)$  and choosing  $\nu_m = 0$ .

Then, for each model, 5000 values of  $\nu'$  were obtained from the maximum likelihood estimates given in (3.29) and by randomly sampling values of  $t_c \sim U(1990, 1990.5)$  and  $\beta \sim U(-1, 0)$  taking a time interval up to 1990 from a starting point drawn randomly from the uniform distribution  $U(1980, 1990)$ . From 5000 values of  $\nu'$  a most likely value  $\bar{\nu}_m$  was determined by using the modeest package in R.

Superexponential growth. For superexponential growth, the procedure was similar to that of normal growth with the crucial difference that  $\nu_m$  were chosen randomly from the distribution (3.10). As before, the model was then simulated 5000 times and a most likely value  $\bar{\nu}_m$  was obtained from the 5000 values of  $\nu'$  calculated from the maximum likelihood estimates (3.28).

Fit generalised logistic distributions and find  $\bar{\nu}_T$ . In both cases, the distributions of  $\{\bar{\nu}_m : m = 1, \dots, 5000\}$  were well described by generalised logistic distributions

as shown in Fig. 5. By examining these distributions,  $\bar{\nu}_T$  was calculated. This is a threshold value which is specifically relevant for the S&P500 index.

Find most likely value of  $\bar{\nu}$  for each trading day of the observed data. Now, for each trading day of the S&P500 index from 1960 up until the present day the distribution of  $\nu'$  was calculated by taking 5000 random samples of the parameters  $t_c$  and  $\beta$  from the same distributions as for the simulated data and applying (3.15) for randomly chosen time periods of up to ten years.

Identify regime change-points. Finally, for each trading day, the calculated value of  $\bar{\nu}$  was compared to the value of  $\bar{\nu}_T$ . Where  $\bar{\nu} \leq \bar{\nu}_T$  it was determined that the market at that point was governed by a superexponential regime.

The results of this process are shown in Fig. 7. From a visual inspection, the areas where it is determined that superexponential growth as the more likely governing regime (as shown in the blue shading) seem to correspond almost exclusively to periods of growth. Encouragingly for the algorithm, we do not detect superexponential growth rates in periods of negative growth, and there are also long periods of actual growth in the market which is not detected as superexponential. This is what one would expect to find based on the initial assumptions.

On closer examination, it appears that, at least when viewed from an ex post perspective, there may be a predictive quality to the algorithm, in that just prior to crashes, steep sell-offs, and longer declines, there are shifts from one regime to the other demonstrated by a well-defined boundary between shaded and subsequently non-shaded areas. These are the change-points that have been sought in the data.

However, as one would expect with observed data, the results are subject to a fair degree of “noise”, in that there are periods of superexponential growth interspersed with brief periods of normal growth. Since it is unlikely that the market governing regime would switch this rapidly, we conclude the algorithm does not capture the granular-level market features, but appears to identify remarkably well the gross features of the market over longer timescales. Note that it appears that longer periods of normal growth are not generally interspersed by shorter periods of superexponential growth.

We now focus on some notable historical financial events, and the results from application of the algorithm over shorter timescales. In particular, we look at the 10-year periods preceding the great crash of October 1987, so called Black Monday, the financial crisis of 2007 – 2009, and the 2015 – 2016 stock market sell-off. These are shown in Fig. 8 as plots (a), (b) and (c) respectively.

Black Monday. The most notable, and well studied, financial crash of the second half of the last century is the stock market crash of Monday, 19 October 1987. There has been much debate over the causes of this crash and the subsequent

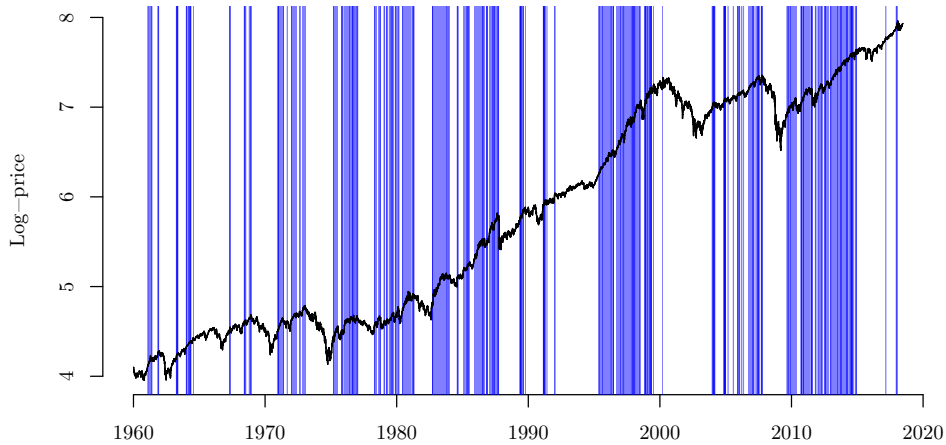


Fig. 7. Results from applying the threshold value,  $\bar{\nu}_T$ , found from the fitted distributions of  $\bar{\nu}$  calculated from both superexponential and normal market simulations, to the historical daily log-returns of the S&P500 index from January 1960 to June 2018. Areas where the calculated value of  $\bar{\nu}$  for the observed data is less than  $\bar{\nu}_T$  are shaded in blue. One can see a striking visual correlation between periods of high growth and the blue shaded area, and also a general agreement between the right boundaries of visually significant areas of blue shading and subsequent market downturns.

contagion across the global financial markets (Barro et al. 1989). When viewed from an econophysics perspective, the crash has often been attributed to critical behaviour following a period of superexponential power-law growth decorated with log-periodic oscillations (Sornette et al. 1996 and Feigenbaum & Freund 1996).

By the method presented here, bearing in mind that, for each point ten years' worth of preceding market data is used, we detect the superexponential growth modelled by the log-periodic power-law models for the period immediately prior to Black Monday. However, there are also periods in which superexponential growth is not detected. Indeed, we see each market rally showing superexponential growth, and when the market is in an intermediate downturn, no superexponential growth is found. There is clearly an oscillatory pattern in the market data, and the algorithm picks up this feature. Furthermore, when looked at closely, with the benefit of hindsight, there are fluctuating periods of sub- and super-threshold regions end some days prior to the crash.

Financial crisis of 2007 – 2009. This period was certainly the worst financial crisis of this century and, probably was the most severe since the Great Depression of

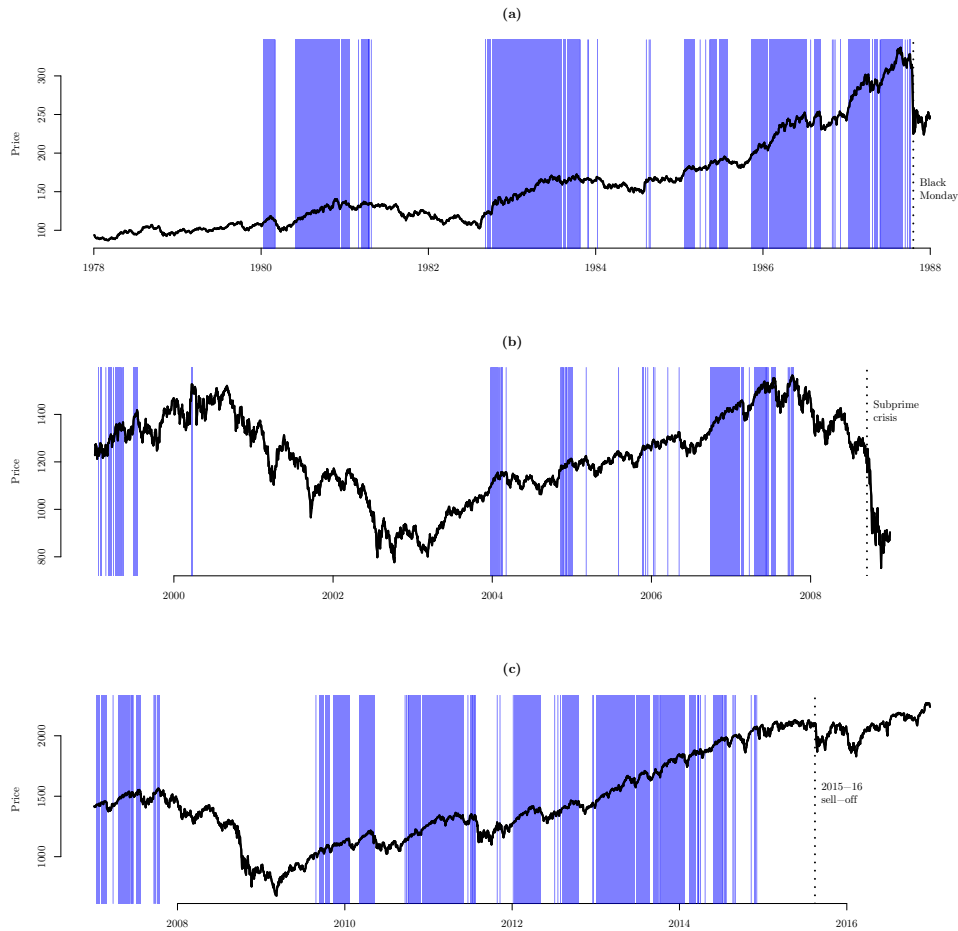


Fig. 8. Results from applying the threshold value,  $\bar{\nu}_T$ , found from the fitted distributions of  $\bar{\nu}$  for specific periods in the last 60 years of the S&P500 index. (a) Black Monday, October 1987, (b) the financial crisis of 2007 – 2009, and (c) the 2015 – 2016 stock market sell-off. Note that for clarity the price rather than the log price is shown.

the 1930s. The US market peaked in October 2007 and there followed a period of steep decline until the global markets suffered a significant draw-down when the fall-out of the subprime mortgage market led to the collapse of large US banking institutions, such as Lehman Brothers, on 15 September 2008. What followed was a global economic downturn, which became known as the Great Recession.

The period 2003 – 2007 was a bull market. However, when we look at the calculated intervals of superexponential growth in this period, we only see sustained superexponential growth from late 2006. Contrary to the example of Black Mon-

day, the superexponential regime does not end with a crash following immediately afterwards, but rather a steep downturn continuing for some time prior to a more severe crash.

2015 – 2016 stock market sell-off. Since the end of the Great Recession in 2009, the market followed an almost relentless bull run up to the end of our observed data (June 2018). This is one of the longest bull markets in history, and, according to our analysis, the majority of it has been governed by a superexponential regime from late 2009 until the beginning of 2015. There does not appear to be the oscillatory patterns of the bull market in the 10 years prior to Black Monday, and, looking at the data from an ex post perspective, it is clear that the superexponential period ended with a relatively long period of growth. Here we see an example of a superexponential bubble, which peters out rather than suffering a catastrophic burst. However, the following August the market did suffer large losses which took until the following June to recover.

These examples show that if there is merit in the algorithm's ability to detect periods where the markets are in a bubble regime and experiencing superexponential growth, the transitioning from one regime to the other is not typified by either a catastrophic crash or a market downturn. However, in general there is a good agreement that market downturns are preceded by a regime change, and this appears to be evident on a variety of scales.

## 5. Conclusion and suggestion for further work

We conclude with some remarks on further study in this area. The distributions of the parameter  $\bar{\nu}$  for the normal and superexponential growth regimes are very well fitted by generalised/skew logistic distributions. Although logistic distributions have been used successfully to model financial assets (Olson & Wu 2013, Tolikas & Gettinby 2009 and Tolikas & Brown 2006), further work is needed to elicit the reason for the logistic distributions in this case. It is worth noting that the logistic distribution is known to arise in extreme value statistics — see Gumbel's classical result on the distribution of the midrange of samples from a continuous distribution (Gumbel 1944).

In the modelling presented herein we have not given a full model of the time series, but rather we have focussed on the influence of the parameter  $\nu$ . Indeed, we have generated simulated data with superexponential mean log-returns and we have specifically constructed the simulations to have constant standard deviations in the stochastic terms. In examining these simulated times series we have restricted to the case of constant  $\sigma_t$ . We conjecture that it is the existence, or otherwise, of the hazard function in the drift term alone that can determine whether regime change has occurred. Although this simplification greatly eases the analysis, allowing a closed-form solution to the log-likelihood minimising value of  $\nu$ , it is to be hoped that



future theoretical developments will provide a more complete theory incorporating time-varying  $\sigma$ .

The financial significance of the parameter  $\bar{\nu}$  needs further study. Formally, it is the coefficient of the hazard function corresponding to a superexponential financial bubble, and it would certainly be interesting to investigate in some detail possible financial interpretations, perhaps leading to further understanding of the distribution of  $\bar{\nu}$ .

The investigations so far have been restricted to the S&P500 index, albeit over 60 years, which constitutes a serious longitudinal study. However, it remains to apply this methodology to other financial time series, including other stock-market indices.

Finally, an important area for future research is the practical utility of the distributions of  $\bar{\nu}$  for financial practitioners. Can  $\bar{\nu}$  be used by traders either for short-term trades (both on the index itself and/or derivatives) or for market timing for longer-term trading strategies? Indeed, can  $\bar{\nu}$  be used as an early-warning for financial crashes and/or the end of a bull market? An in-depth study of these and other issues would be of significant interest to practitioners and theoreticians alike.

## References

- Adams, R. P. & MacKay, D. J. C. (2007). Bayesian Online Changepoint Detection, arXiv 0710.3742 [unpublished].
- Aminikhanghahi, S. & Cook, D. J. (2017). A survey of methods for time series change point detection, *Knowledge and Information Systems* 51(2): 339–367.
- Arshanapalli, B. & Nelson, W. (2016). Testing for Stock Price Bubbles: a Review of Econometric Tools, *The International Journal of Business and Finance Research* 10(4): 29–42.
- Astill, S., Harvey, D. I., Leybourne, S. J. & Taylor, A. M. (2017). Tests for an end-of-sample bubble in financial time series, *Econometric Reviews* 36(6-9): 651–666.
- Barro, R. J., Kormendi, R. C., Kamphuis, R. W. & Watson, J. W. H. (1989). Black Monday and the future of financial markets / Robert J. Barro ... [et al.] ; edited by Robert W. Kamphuis, Jr., Roger C. Kormendi, and J.W. Henry Watson, Dow Jones-Irwin ; Mid America Institute for Public Policy Research, Inc Homewood, Ill. : Chicago, Ill.
- Benson, A. & Friel, N. (2018). Adaptive MCMC method for multiple changepoint analysis with applications to large datasets, *Electron. J. Statist* 12(2): 3365–3396.
- Cheah, E.-T. & Fry, J. (2015). Speculative bubbles in bitcoin markets? An empirical investigation into the fundamental value of bitcoin, *Economics Letters* 130: 32 – 36.
- Feigenbaum, J. A. & Freund, P. G. O. (1996). Discrete scale invariance in stock markets before crashes, *International Journal of Modern Physics B* 10: 3737–3745.
- Gumbel, E. J. (1944). Ranges and Midranges, *The Annals of Mathematical Statistics* 15(4): 414–422.
- Gürkaynak, R. S. (2008). Econometric tests of asset price bubbles: taking stock, *Journal of Economic Surveys* 22(1): 166–186.
- Harvey, D. I., Leybourne, S. J. & Sollis, R. (2015). Recursive Right-Tailed Unit Root Tests for an Explosive Asset Price Bubble, *Journal of Financial Econometrics* 13(1): 166–187.
- Heard, N. A. & Turcotte, M. J. M. (2017). Adaptive Sequential Monte Carlo for Mul-

- multiple Changepoint Analysis, *Journal of Computational and Graphical Statistics* 26(2): 414–423.
- Jackson, B., Scargle, J., Barnes, D., Arabhi, S., Alt, A., Gioumousis, P., Gwin, E., San, P., Tan, L. & Tun Tao Tsai (2005). An algorithm for optimal partitioning of data on an interval, *IEEE Signal Processing Letters* 12(2): 105–108.
- Jarrow, R. (2016). Testing for asset price bubbles: three new approaches, *Quantitative Finance Letters* 4(1): 4–9.
- Johansen, A., Ledoit, O. & Sornette, D. (2000). Crashes as critical points, *International Journal of Theoretical and Applied Finance* 03(02): 219–255.
- Killick, R. & Eckley, I. (2013). changepoint: An R Package for changepoint analysis, *Journal of Statistical Software* 58(3): 1–15.
- Killick, R., Fearnhead, P. & Eckley, I. A. (2012). Optimal detection of changepoints with a linear computational cost, *Journal of the American Statistical Association* 107(500): 1590–1598.
- Mills, T. C. & Markellos, R. N. (2008). *The econometric modelling of financial time series*, Cambridge University Press.
- Olson, D. L. & Wu, D. (2013). The impact of distribution on value-at-risk measures, *Mathematical and Computer Modelling* 58: 1670–1676.
- Robertson, D. & Wright, S. M. (1998). The good news and the bad news about long-run stock market returns, *Cambridge Working Papers in Economics* 10.17863/CAM.5034.
- Sornette, D., Johansen, A. & Bouchaud, J. (1996). Stock market crashes, precursors and replicas, *Journal de Physique I* 6(1): 167–175.
- Taipalus, K. (2012). Detecting asset price bubbles with time-series methods, *Scientific Monographs*, Bank of Finland E:47.
- Tolikas, K. & Brown, R. A. (2006). The distribution of the extreme daily share returns in the Athens stock exchange, *The European Journal of Finance* 12(1): 1–22.
- Tolikas, K. & Gettinby, G. D. (2009). Modelling the distribution of the extreme share returns in Singapore, *Journal of Empirical Finance* 16(2): 254–263.